

AdvantageFlow: Advantage-Weighted Least Squares for RL in Flow Models

Branislav Kveton, Anup Rao, Subhojyoti Mukherjee, Krishna Kumar Singh, Viet Dac Lai
 Adobe Research
 kveton@adobe.com

Abstract

We introduce AdvantageFlow, a forward-process reinforcement learning algorithm for rectified flow models. Unlike Flow-GRPO, which optimizes the reverse process, we optimize an advantage-weighted forward-process prediction loss. This optimization problem is unstable when advantages are negative and the loss becomes non-convex. We stabilize it by rollout policy regularization, which reduces variance and arises from fitting a local reward-improving target distribution. We evaluate AdvantageFlow on image generation tasks with Stable Diffusion 3.5 Medium. It outperforms both Flow-GRPO and a state-of-the-art forward-process RL baseline based on negative-aware fine-tuning.



Figure 1: Images generated by [AdvantageFlow\(1.1\)](#) compared to [DiffusionNFT](#) and base model (Stable Diffusion 3.5 Medium) with cfg. [AdvantageFlow](#) improves in generating objects, counting, color understanding, and position understanding; all without classifier free guidance (cfg). These results are obtained after 125 H100 GPU training hours.

1 Introduction

Flow and diffusion models are standard models for generating high-quality images [[Lipman et al., 2023](#), [Liu et al., 2023](#), [Albergo et al., 2023](#)]. The models are usually pre-trained by minimizing the flow-matching loss and then post-trained to improve human preference alignment, prompt following,

text rendering, and image composition. Given a pre-trained image generation model and a reward model, we want to adapt the pre-trained model to generate more rewarding images, while preserving its quality and diversity. At inference time, images are generated by sampling noise and following a learned denoising trajectory.

Most *reinforcement learning (RL)* algorithms for flow models optimize this sampling process by treating image generation as a sequential process along the reverse denoising trajectory and apply a variant of policy gradients [Black et al., 2024, Fan et al., 2023, Liu et al., 2025a, Clark et al., 2024, Prabhudesai et al., 2023, Domingo-Enrich et al., 2024]. These methods are powerful but complex. They need to introduce additional stochasticity just to compute policy gradients. Moreover, since only the final generated image is rewarded, reward attribution to intermediate denoising steps where mistakes happen must be learned from data. Several recent papers try to improve reward attribution in RL for flow models [Savani et al., 2026, He et al., 2025, Zhou et al., 2025]. Forward-process RL offers a simpler alternative. Instead of optimizing along the reverse sampling process, we sample complete images, score them with rewards, and train the model using the same forward-process loss as in pre-training but with reward-dependent weights. The only change is in the weighting.

We introduce **AdvantageFlow**, a forward-process RL algorithm for rectified flow models. The key idea is to sample a batch of images per prompt and compute their advantages: how much better or worse each image is relative to the batch average. Then we train the model to generate images with higher advantages more frequently, while regularizing it with respect to its moving average to keep the updates stable. The optimized loss function is *advantage-weighted least squares*. The advantage weighting corresponds to fitting a local linearly tilted target distribution that shifts probability mass towards more rewarding samples. The regularization arises naturally as a variance reduction step: it replaces noisy per-sample targets with their conditional means in the reward-independent part of the loss. It also ensures that the loss is strictly convex per sample. We evaluate **AdvantageFlow** on image generation tasks with Stable Diffusion 3.5 Medium. **AdvantageFlow** improves the quality of generated images for several reward models and can also be applied to multi-objective optimization. It outperforms both **Flow-GRPO** [Liu et al., 2025a] and a state-of-the-art forward-process RL baseline based on negative-aware fine-tuning [Zheng et al., 2026]. We complement our evaluation by GenEval [Ghosh et al., 2023] to mitigate a potential concern of reward hacking.

Our contributions are: (1) We introduce **AdvantageFlow**, a least-squares algorithm for reinforcement learning in flow models using the forward process. (2) We derive the algorithm from a local reward-improving target distribution, where the rollout regularization arises as a variance reduction technique for noisy sampled targets. (3) We show that a state-of-the-art algorithm for forward-process RL is an instance of our method with a particular adaptive rollout regularization. (4) We empirically evaluate **AdvantageFlow** on image generation tasks with Stable Diffusion 3.5 Medium. We observe that it generates high-quality images and outperforms state-of-the-art baselines.

2 Background

We briefly review flow matching for image generation [Lipman et al., 2023, Liu et al., 2023, Albergo et al., 2023]. *Rectified flow matching models* learn continuous-time normalizing flows by training on a linear interpolation of clean images and Gaussian noise. Let c be a prompt and $q(\cdot | c)$ be a distribution over clean images. Let $x_0 \sim q(\cdot | c)$ be a random clean image, $\epsilon \sim \mathcal{N}(0, I)$ be Gaussian noise, and $t \sim [0, 1]$ be a random time. Then the flow matching objective is minimizing

$$\mathbb{E}_{x_0 \sim q(\cdot | c), \epsilon, t} [\|v_\theta(x_t, t, c) - (\epsilon - x_0)\|_2^2], \quad (1)$$

where $x_t = (1 - t)x_0 + t\epsilon$ is a random interpolation of x_0 and ϵ , $v_\theta(x_t, t, c)$ is the *predicted velocity* at x_t , θ is the *learned model parameter*, and $\epsilon - x_0$ is the ground-truth velocity. The objective (1) can also be viewed as prediction loss minimization. Specifically, the *predicted clean image* at x_t is $f_\theta(x_t, t, c) = x_t - t v_\theta(x_t, t, c)$ and hence $\|f_\theta(x_t, t, c) - x_0\|_2^2 = t^2 \|v_\theta(x_t, t, c) - (\epsilon - x_0)\|_2^2$.

Because of this equivalence, the theory in this work could be done for both the velocity loss in (1) or prediction loss, which differs only by t^2 . We focus on the latter due to better empirical performance. Our goal is to develop and justify algorithms for minimizing

$$\mathbb{E}_{x_0 \sim q(\cdot | c), \epsilon, t} [\|f_\theta(x_t, t, c) - x_0\|_2^2] \quad (2)$$

weighted by rewards. Without the rewards, the minimizer is the conditional mean of x_0 .

Sampling in flow models is implemented using a *deterministic ODE*. Specifically, it starts with noise x_T and follows a denoising *trajectory* $x_T, x_{T-\Delta t}, \dots, x_0$, where

$$x_{t-\Delta t} = x_t - v_\theta(x_t, t, c) \Delta t. \quad (3)$$

The key idea in most existing RL algorithms for flow models, such as **Flow-GRPO**, is treating this trajectory as a sequential process with *reward* $r(x_0, c)$, for final generated image x_0 given prompt c . There are two challenges. The first challenge is that policy gradients [Williams, 1992] cannot be applied to deterministic trajectories, such as the one generated by (3). To address this, **Flow-GRPO** replaces (3) with an SDE

$$x_{t-\Delta t} = x_t - \left[v_\theta(x_t, t, c) - \frac{\sigma_t^2}{2t} \hat{x}_1 \right] \Delta t + \sigma_t \sqrt{\Delta t} \xi, \quad \hat{x}_1 = x_t + (1-t) v_\theta(x_t, t, c), \quad (4)$$

where $\xi \sim \mathcal{N}(0, I)$ and σ_t is the noise schedule of the stochastic sampler. This defines a Gaussian transition $\pi_\theta(x_{t-\Delta t} | x_t, c)$ at denoising step t with covariance $\sigma_t^2 \Delta t I$, allowing policy gradients to be applied. The second challenge is that the reward $r(x_0, c)$ is assigned only to the final generated image, while $\pi_\theta(x_{t-\Delta t} | x_t, c)$ needs to be optimized. This creates a reward attribution problem and many recent works try to improve it [Savani et al., 2026, He et al., 2025, Zhou et al., 2025].

Forward-process RL has neither of these problems. It uses the ODE sampler in (3) to generate clean images and thus is better aligned with the inference-time denoising. The clean image is predicted directly using $f_\theta(x_t, t, c)$ and therefore no reward attribution is needed.

3 Algorithm

We introduce **AdvantageFlow**, a forward-process RL algorithm for rectified flow models. The key idea is to minimize the prediction loss in (2) weighted by advantages. The optimization of the loss is stabilized by regularization by a *rollout policy*, which generates images and is slowly updated. To prevent the loss of capabilities that we do not optimize for, we additionally regularize by a *reference policy*. We denote the predictions of clean images under the learned, rollout, and reference policies by f_θ , f_{old} , and f_{ref} , respectively.

3.1 Intuition

Suppose that we sample multiple images per prompt and score them with rewards. Some images are better than the average and some are worse. We want to generate the good images more often than the bad ones. A natural idea is to minimize the prediction loss in (2) weighted by advantages, rewards minus the mean reward, which upweight above-average images and downweight the rest. Specifically, the loss in (2) becomes $A(x_0, c) \|f_\theta(x_t, t, c) - x_0\|_2^2$, where $A(x_0, c)$ is the *advantage* of clean image x_0 given prompt c .

This alone is not sufficient. When an image has a negative advantage, $A(x_0, c) \|f_\theta(x_t, t, c) - x_0\|_2^2$ becomes negative. This can lead to ill-conditioned optimization and divergence because the loss is not convex in f_θ anymore. To fix it, we regularize $f_\theta(x_t, t, c)$ by a prediction under the rollout policy, $f_{\text{old}}(x_t, t, c)$. This stabilizes the optimization and keeps the update local with respect to the rollout policy. In addition, we regularize $f_\theta(x_t, t, c)$ by a prediction under the reference policy, $f_{\text{ref}}(x_t, t, c)$. This prevents the learned policy from losing capabilities not captured by rewards. Putting all of these together, our objective is

$$\mathbb{E}_{x_0 \sim p_{\text{old}}(\cdot|c), \epsilon, t} [\ell_{\theta, \theta_{\text{old}}}(A(x_0, c), x_0, x_t, t, c)], \quad (5)$$

where $\ell_{\theta, \theta_{\text{old}}}(A(x_0, c), x_0, x_t, t, c) =$

$$A(x_0, c) \|f_\theta(x_t, t, c) - x_0\|_2^2 + \gamma \|f_\theta(x_t, t, c) - f_{\text{old}}(x_t, t, c)\|_2^2 + \lambda \|f_\theta(x_t, t, c) - f_{\text{ref}}(x_t, t, c)\|_2^2.$$

We refer to the three terms as the advantage-weighted prediction loss, rollout regularization, and reference regularization. The weights $\gamma, \lambda \geq 0$ control the amount of rollout and reference regularization, respectively.

The loss inside (5) has three terms with the following functions. The *advantage-weighted prediction loss* fits the policy to the generated images weighted by their advantages. Positive $A(x_0, c)$ pull the

Algorithm 1 AdvantageFlow

- 1: **Input:** Pre-trained model θ_{ref} , reward model r , prompt dataset \mathcal{C} , batch size L , group size K , regularization strengths $\gamma, \lambda \geq 0$, and EMA update rate $\rho \geq 0$
 - 2: Initialize $\theta \leftarrow \theta_{\text{ref}}$ and $\theta_{\text{old}} \leftarrow \theta_{\text{ref}}$
 - 3: **for** each iteration **do**
 - 4: Sample L prompts $c_1, \dots, c_L \sim \mathcal{C}$
 - 5: For each c_i , generate K images $x_0^{i,1}, \dots, x_0^{i,K}$ using (3) with rollout velocity v_{old}
 - 6: **for all** $(i, k) \in [L] \times [K]$ **do**
 - 7: Compute per-image advantage $A^{i,k}$ using (6)
 - 8: $x_t^{i,k} \leftarrow (1 - t^{i,k}) x_0^{i,k} + t^{i,k} \epsilon^{i,k}$, for freshly sampled $t^{i,k}$ and $\epsilon^{i,k}$
 - 9: Update θ by gradient descent on $\frac{1}{KL} \sum_{i=1}^L \sum_{k=1}^K \ell_{\theta, \theta_{\text{old}}}(A^{i,k}, x_0^{i,k}, x_t^{i,k}, t^{i,k}, c_i)$
 - 10: Update rollout policy as $\theta_{\text{old}} \leftarrow \rho \theta_{\text{old}} + (1 - \rho) \theta$
 - 11: **Output:** θ
-

policy towards good images and negative $A(x_0, c)$ push it away from the bad images. The *rollout regularization* penalizes deviations from the rollout policy. It ensures that the loss is strictly convex per sample, by making the total quadratic coefficient $A(x_0, c) + \gamma + \lambda$ positive (Section 3.3). The *reference regularization* penalizes deviations from the initial pre-trained model. It prevents forgetting behaviors not captured by the reward.

3.2 AdvantageFlow

Our algorithm is iterative. At each iteration, we sample L prompts, generate K images per prompt using the rollout policy, score the images by rewards, compute their advantages, and then update the learned and rollout policies. We call the algorithm **AdvantageFlow** because it optimizes the flow model using advantages. The pseudo-code is in Algorithm 1.

Sampling. The images are sampled from the rollout policy. The policy is parameterized by θ_{old} , which has the same dimensionality as the learned policy parameter θ . The parameter θ_{old} is slowly updated using an *exponential moving average (EMA)* of θ , motivated by Zheng et al. [2026]. Both θ and θ_{old} parametrize velocity models v_θ and v_{old} . Therefore, they can be used to sample images, through (3), or predict clean images, through f_θ and f_{old} .

Advantages. The advantages can be computed in many ways [Shao et al., 2024, Liu et al., 2025b,a]. Inspired by Zheng et al. [2026], we standardize them per-batch as follows. Let $r^{i,k}$ be the reward for image $k \in [K]$ and prompt c_i , where $i \in [L]$. Then the corresponding advantage is

$$A^{i,k} = \text{clip} \left(\frac{r^{i,k} - \hat{r}^i}{Z}, -1, 1 \right), \quad \hat{r}^i = \frac{1}{K} \sum_{k=1}^K r^{i,k}, \quad Z = \sqrt{\frac{1}{KL} \sum_{i=1}^L \sum_{k=1}^K (r^{i,k} - \hat{r}^i)^2}, \quad (6)$$

where \hat{r}^i is the per prompt mean and Z is the batch standard deviation. The advantage of a sample is positive if its reward is above the average and negative if it is below.

Prediction loss minimization. We minimize an empirical version of (5), where the expectation over prompts, clean images, time, and Gaussian noise is approximated by an empirical average over KL samples in a batch. The time t and noise ϵ are drawn fresh per sample.

Computational cost. Each iteration of **AdvantageFlow** scales linearly with the number of samples per batch KL . This is due to sampling KL images using v_{old} and minimizing an empirical prediction loss over them, requiring predictions by f_θ , f_{old} , and f_{ref} for each noisy image $x_t^{i,k}$.

Space complexity. The space complexity is mostly driven by the dimensionality of θ and θ_{old} . In our work, both are encoded using LoRA [Hu et al., 2022] on the top of the initial pre-trained model, which represents the reference policy. We also store KL generated images and their advantages in each iteration.

3.3 Strict Convexity and Algorithmic Variants

The loss inside (5) is quadratic in f_θ for any sample, with a *quadratic coefficient* $A(x_0, c) + \gamma + \lambda$. It is strictly convex, and therefore has a unique minimum in the prediction space when

$$A(x_0, c) + \gamma + \lambda > 0. \quad (7)$$

Without rollout regularization, $\gamma = 0$ and negative advantages $A(x_0, c)$ could make the quadratic coefficient negative, thus turning the loss concave and making optimization unstable.

Since the advantages in (6) are clipped to $[-1, 1]$, it is easy to ensure that (7) holds for each sample: any $\gamma > 1$ suffices, irrespective of $\lambda \geq 0$. We experiment with two choices. A non-adaptive $\gamma = 1.1$ keeps the total quadratic coefficient close to $\gamma + \lambda$ across the batch, since the unclipped advantage is centered and clipping keeps the coefficient bounded. We call this algorithm [AdvantageFlow\(1.1\)](#). On the other hand, the advantage-dependent choice $\gamma(A) = 1 - A(x_0, c)$ guarantees that the total quadratic coefficient is $A(x_0, c) + \gamma(A) + \lambda = 1 + \lambda$ per sample and thus constant. We call this algorithm [AdvantageFlow\(1-A\)](#) and relate it to [DiffusionNFT](#) in Section 4.4.

4 Analysis

We now show that the [AdvantageFlow](#) objective arises from fitting a local reward-improving target distribution, with the rollout policy entering as a variance reduction step. We also show that [DiffusionNFT](#) can be viewed as a special case of [AdvantageFlow](#). Our analysis below is local and under exact expectations.

4.1 Linearly Tilted Target Distribution

Fix a prompt c and let $p_{\text{old}}(\cdot | c)$ be the rollout distribution. We define the centered advantage

$$A(x_0, c) = r(x_0, c) - \mathbb{E}_{x'_0 \sim p_{\text{old}}(\cdot | c)}[r(x'_0, c)]. \quad (8)$$

Consider the distribution obtained by tilting p_{old} by a factor linear in the advantage,

$$q_\eta(x_0 | c) = (1 + \eta A(x_0, c)) p_{\text{old}}(x_0 | c). \quad (9)$$

It increases the probability of above-average samples ($A(x_0, c) > 0$) and decreases that of below-average samples ($A(x_0, c) < 0$), proportionally to how far each sample is from the mean reward. Since the advantage is centered, $\mathbb{E}_{x_0 \sim p_{\text{old}}(\cdot | c)}[A(x_0, c)] = 0$, the perturbation integrates to zero and q_η is automatically normalized: $\int q_\eta(x_0 | c) dx_0 = \int p_{\text{old}} dx_0 + \eta \int A p_{\text{old}} dx_0 = 1 + 0 = 1$. If $1 + \eta A(x_0, c) \geq 0$ for all x_0 (equivalently, the rescaled form of the pointwise positivity condition $A + \gamma > 0$ from Section 3.3 with $\gamma = 1/\eta$ and $\lambda = 0$), $q_\eta(x_0 | c) \geq 0$ and therefore a valid probability distribution. It also improves the expected reward by $\eta \text{Var}_{p_{\text{old}}(\cdot | c)}(r(\cdot, c)) \geq 0$, since $\mathbb{E}_{q_\eta}[r] - \mathbb{E}_{p_{\text{old}}}[r] = \eta \mathbb{E}_{p_{\text{old}}}[Ar] = \eta \mathbb{E}_{p_{\text{old}}}[A^2] = \eta \text{Var}_{p_{\text{old}}}(r)$, using $\mathbb{E}_{p_{\text{old}}}[A] = 0$ and the definition of variance. The linear tilt q_η in (9) is the first-order natural-gradient update for maximizing expected reward under the Fisher-Rao metric on probability distributions [[Amari, 1998](#), [Kakade, 2001](#)]. We make this connection precise.

Proposition 1 (Fisher-Rao natural-gradient direction). *Fix a prompt c and let $F(p) = \mathbb{E}_p[r(\cdot, c)]$. Under the Fisher-Rao metric, the natural-gradient direction of F at $p = p_{\text{old}}(\cdot | c)$ is the tangent vector*

$$\delta p(x_0) = A(x_0, c) p_{\text{old}}(x_0 | c), \quad A(x_0, c) = r(x_0, c) - \mathbb{E}_{p_{\text{old}}(\cdot | c)}[r(\cdot, c)].$$

A first-order step of size η along this direction yields the additive tilt $q_\eta(\cdot | c) = (1 + \eta A(\cdot, c)) p_{\text{old}}(\cdot | c)$ from (9).

The proof is in Section B. The Fisher-Rao metric is the canonical Riemannian metric on probability distributions and underlies natural policy gradient methods in reinforcement learning [[Kakade, 2001](#)]. Proposition 1 carries this picture over to flow models: [AdvantageFlow](#) can be read as natural-gradient ascent on expected reward, with the rollout distribution as the base point and η as the step size.

4.2 Advantage-Weighted Loss

To move the learned policy towards q_η , we minimize the prediction loss against it,

$$\mathcal{L}_{q_\eta}(\theta) = \mathbb{E}_{x_0 \sim q_\eta(\cdot|c), \epsilon, t} [\|x_0 - f_\theta(x_t, t, c)\|_2^2]. \quad (10)$$

Changing measure to samples from p_{old} gives

$$\mathcal{L}_{q_\eta}(\theta) = \mathbb{E}_{x_0 \sim p_{\text{old}}, \epsilon, t} [(1 + \eta A) \|x_0 - f_\theta(x_t, t, c)\|_2^2], \quad (11)$$

where the dependence of A on x_0, c is suppressed. Expanding the weight separates these into

$$\mathcal{L}_{q_\eta}(\theta) = \underbrace{\mathbb{E}_{x_0 \sim p_{\text{old}}, \epsilon, t} [\|x_0 - f_\theta(x_t, t, c)\|_2^2]}_{\text{reward-independent}} + \eta \underbrace{\mathbb{E}_{x_0 \sim p_{\text{old}}, \epsilon, t} [A \|x_0 - f_\theta(x_t, t, c)\|_2^2]}_{\text{reward-dependent}}. \quad (12)$$

Only the reward-dependent term distinguishes good samples from bad. The reward-independent term is ordinary flow matching on samples from p_{old} . It pulls the policy towards the rollout distribution but does not use reward values.

4.3 Variance Reduction by Rollout Policy

Variance reduction in policy optimization is a well-studied topic [Sutton et al., 2000, Baxter and Bartlett, 2001, Munos, 2006]. The reward-independent term is defined on individual samples x_0 , but the population minimizer of this term is the conditional mean $\mathbb{E}_{x_0 \sim p_{\text{old}}, \epsilon} [x_0 | x_t, t, c]$. If the rollout policy is well-trained, its prediction $f_{\text{old}}(x_t, t, c)$ approximates this conditional mean. We then are better off by replacing x_0 with the prediction $f_{\text{old}}(x_t, t, c)$ in reward-independent term of Equation (12).

Proposition 2 (Variance reduction). *Fix a prompt c and suppose $f_{\text{old}}(x_t, t, c) = \mathbb{E}_{x_0 \sim p_{\text{old}}(\cdot|c), \epsilon} [x_0 | x_t, t, c]$. Up to a θ -independent constant,*

$$\mathbb{E}_{x_0 \sim p_{\text{old}}, \epsilon, t} [\|x_0 - f_\theta(x_t, t, c)\|_2^2] = \mathbb{E}_{x_0 \sim p_{\text{old}}, \epsilon, t} [\|f_{\text{old}}(x_t, t, c) - f_\theta(x_t, t, c)\|_2^2].$$

Moreover, the single-sample gradient of the right-hand side has no larger variance than that of the left-hand side.

The proof is in Section C. The key observation is that x_0 is a single noisy draw from $p_{\text{old}}(\cdot | c)$, while $f_{\text{old}}(x_t, t, c)$ is trained to match its conditional mean. Using f_{old} as the regression target removes sample noise. The population minimizer is unchanged, and the gradient estimator is lower-variance by the Rao-Blackwell argument [Casella and Robert, 1996]. Substituting this into (12) and rescaling by $\eta = 1/\gamma$ gives the objective of **AdvantageFlow** in Section 3 without reference regularization,

$$\mathbb{E}_{x_0 \sim p_{\text{old}}, \epsilon, t} [A(x_0, c) \|x_0 - f_\theta(x_t, t, c)\|_2^2 + \gamma \|f_\theta(x_t, t, c) - f_{\text{old}}(x_t, t, c)\|_2^2]. \quad (13)$$

4.4 Connection to DiffusionNFT

DiffusionNFT is arguably the first forward-process RL algorithm for flow models with impressive empirical results [Zheng et al., 2026]. Our work differs from it in several aspects, which we want to highlight first.

First, a major gap between theoretical justification of **DiffusionNFT** and its implementation exists. Specifically, the velocity losses of implicit positive and negative policies, which are analyzed, are replaced by adaptively-weighted prediction losses when implemented. In contrast, **AdvantageFlow** is both analyzed (Section 4) and implemented (Section 3) with prediction losses. Second, the loss of **DiffusionNFT** is derived based on preference between implicit positive and negative samples. In contrast, the **AdvantageFlow** loss is derived from the first principles, directly from the objective of reward-weighted flow loss minimization (Section 4). This yields an embarrassingly simple algorithm that works well empirically (Section 5). Finally, **DiffusionNFT** is analyzed using the velocity loss while our analysis uses the prediction loss.

AdvantageFlow and **DiffusionNFT** can also be related as follows: replace the velocity losses in **DiffusionNFT** by prediction losses, expand the squares of implicit positive and negative policies, and drop the terms independent of θ . Then we get (Section D)

$$\beta A(x_0, c) \|x_0 - f_\theta(x_t, t, c)\|_2^2 + \gamma_{\text{NFT}}(A) \|f_\theta(x_t, t, c) - f_{\text{old}}(x_t, t, c)\|_2^2, \quad (14)$$

where $\gamma_{\text{NFT}}(A) = \beta(\beta - A(x_0, c))$. For $\beta = 1$, $\gamma_{\text{NFT}}(A) = 1 - A(x_0, c)$ and the loss becomes a special case of (5), where $\lambda = 0$ and the rollout regularizer is chosen adaptively, as in Section 3.3.

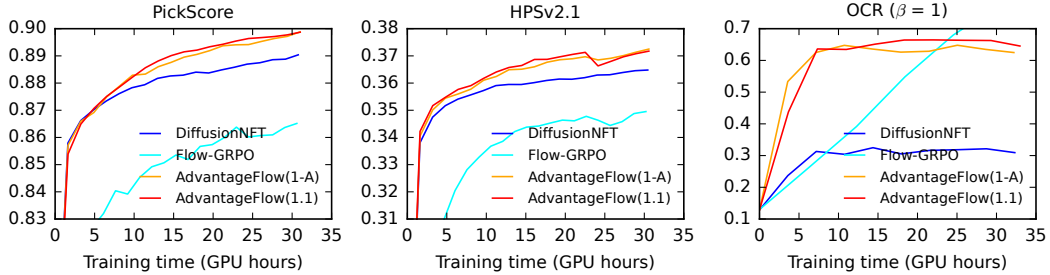


Figure 2: Evaluation of **AdvantageFlow**, **DiffusionNFT**, and **Flow-GRPO** on **PickScore**, **HPSv2.1**, and **OCR**. All rewards are measured on test sets and reported as a function of training time.

5 Experiments

We experiment with 512×512 images generated by Stable Diffusion 3.5 Medium [Esser et al., 2024]. All experiments are implemented in the **DiffusionNFT** code base¹ [Zheng et al., 2026], which is based on that of Liu et al. [2025a]. We consider two kinds of reward models: rule- and model-based. *OCR* is ruled-based and evaluates text rendering. *GenEval* [Ghosh et al., 2023] is ruled-based and evaluates image composition. *PickScore* [Kirstain et al., 2023], *HPSv2.1* [Wu et al., 2023], and *CLIPScore* [Hessel et al., 2021] are learned reward models that measure image quality, text-to-image alignment, and human preference. For *OCR*, we use the corresponding training and test sets. For all other reward models, we use the Pick-a-Pic dataset [Kirstain et al., 2023].

We experiment with two variants of **AdvantageFlow** from Section 3.3: **AdvantageFlow(1.1)** with non-adaptive rollout regularization and **AdvantageFlow(1-A)** with the adaptive one. We compare them to **Flow-GRPO** [Liu et al., 2025a] and **DiffusionNFT** [Zheng et al., 2026]. All algorithms are trained on 10 denoising steps (SDE in **Flow-GRPO** and ODE in the others) and evaluated on 40. The learned and rollout policies are implemented by LoRA with $\alpha = 64$ and $r = 32$. We depart from the original experiments of Zheng et al. [2026] only by having an effective batch size 128: 32 prompts with 4 samples per prompt. The number of prompts is comparable (1.5 times lower) but the number of samples is 6 times lower. This gives us a similar prompt coverage at a much lower computational cost. We run all algorithms for 1 000 steps. Each run takes up to 35 H100 GPU hours and all runs can be reproduced in a week on a single H100 node with 8 GPUs. Despite this, we observe similar trends to Zheng et al. [2026]. To reduce the variability of runs, we set the reference regularization strength, in both **AdvantageFlow** and **DiffusionNFT**, to $\lambda = 0.001$. We conduct one larger-scale experiment, for 125 H100 GPU hours, in Section A.

Baseline comparison. We start by comparing **AdvantageFlow** to **DiffusionNFT** and **Flow-GRPO**. Our results are reported in Figure 2, and we observe two main trends. First, **AdvantageFlow(1-A)** outperforms **DiffusionNFT**: it attains the highest reward of **DiffusionNFT** in half the training time on both **PickScore** and **HPSv2.1**. For **OCR**, it attains twice the reward. This shows that despite the similarities (Section 4.4), the direct optimization of the prediction loss in **AdvantageFlow** yields major benefits. Second, **AdvantageFlow(1.1)** performs a bit better than **AdvantageFlow(1-A)**. This suggests that forward-process RL in flow models is stabilized by *rollout policy regularization*, not necessarily adaptive (Section 4.4). Finally, **Flow-GRPO** performs the worst in all experiments but the last one, which is consistent with the results in Zheng et al. [2026].

The original **OCR** experiment in Zheng et al. [2026] is with **DiffusionNFT** for $\beta = 0.1$. We repeat it in Figure 3c, where the prediction and rollout coefficients in **AdvantageFlow** are set accordingly (Section 4.4). After this, **AdvantageFlow(0.01-0.1A)** performs similarly to **DiffusionNFT**, and both outperform **Flow-GRPO**. In all remaining experiments, we only compare to **DiffusionNFT**, the best baseline so far.

Multi-objective optimization. We also experiment with optimizing multiple rewards by training on the sum of **PickScore**, **HPSv2.1**, and **CLIPScore**. We report our results for the combined reward in Figure 3a and the individual rewards in Figure 4. We observe two main trends. First, although we optimize the combined reward, we maximize each individual reward in Figure 4. This shows that

¹<https://github.com/NVlabs/DiffusionNFT>

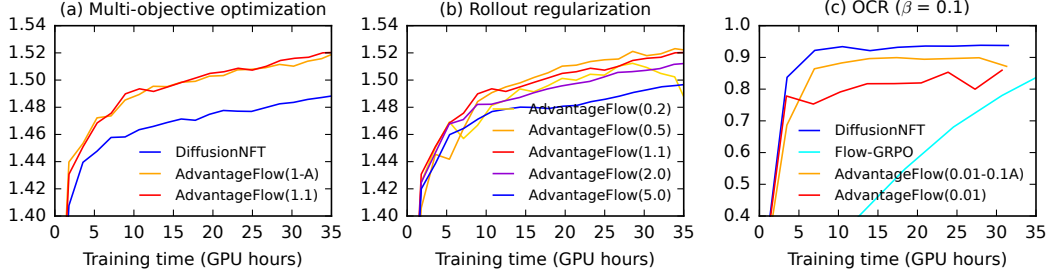


Figure 3: Multi-objective experiments and additional ablation studies. All rewards are measured on test sets and reported as a function of training time.

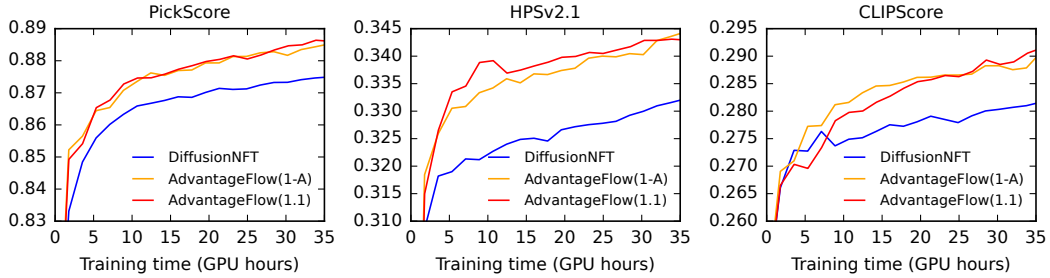


Figure 4: Evaluation of [AdvantageFlow](#) and [DiffusionNFT](#) on multi-objective optimization. We optimize the sum of PickScore, HPSv2.1, and CLIPScore. All rewards are measured on test sets and reported as a function of training time.

simple variants of our method can be used for multi-objective optimization. Second, both variants of [AdvantageFlow](#) attain the highest reward of [DiffusionNFT](#) in less than half the training time. We conduct a larger-scale version of this experiment, where the number of samples per prompt increases to 16, in Section A. We observe that both variants of [AdvantageFlow](#) attain the highest reward of [DiffusionNFT](#) in less than a third training time. We show several examples of image generation improvements in Figure 1 and more in Section A.

Rollout regularization strength. The main tunable parameter of [AdvantageFlow](#) is the strength of rollout regularization. In Figure 3b, we vary it from 0.2 to 5, and observe that the performance drops when the strength is either too low or too high. The former leads to instability and the latter slows down the learning. The highest reward is attained when the strength is close to one. This is the setting in all our experiments but those in Figure 3c. We do not experiment with the reference regularization strength λ because this term is standard in reinforcement learning.

GenEval evaluation. One potential concern about the gains in Figures 2 and 3 is that they are due to reward hacking. To mitigate this concern, we evaluate the policies from Figure 3a using GenEval [Ghosh et al., 2023]. Our results are reported in Table 1 and we observe the following trends. First, [AdvantageFlow](#) improves over the original base model, with or without *classifier-free guidance* (*cfg*). Second, [AdvantageFlow](#) without *cfg* outperforms the base model with *cfg*. This is a testament to the ability of RL to learn highly non-trivial policies through reward maximization. Finally, we note that [AdvantageFlow](#) performs generally at least as well as [DiffusionNFT](#).

6 Related Work

Reward fine-tuning of diffusion and flow models has developed along three lines: trajectory-level RL on the reverse sampling process, reward backpropagation through the sampler, and forward-process RL on scored samples. [AdvantageFlow](#) belongs to the third family. We briefly describe each and then discuss the closest forward-process methods. See Uehara et al. [2024] for a broader review of RL-based fine-tuning of generative models.

Method	Single object	Two objects	Counting	Color	Position	Color binding	Overall
Without cfg							
Base	0.743	0.217	0.128	0.454	0.045	0.102	0.268
DiffusionNFT	0.971	0.795	0.609	0.787	0.242	0.495	0.638
AdvantageFlow(1-A)	0.975	0.835	0.596	0.832	0.247	0.600	0.671
AdvantageFlow(1.1)	0.984	0.863	0.737	0.837	0.260	0.592	0.700
With cfg							
Base	0.978	0.767	0.534	0.789	0.212	0.490	0.617
DiffusionNFT	0.978	0.896	0.693	0.811	0.325	0.572	0.702
AdvantageFlow(1-A)	0.987	0.929	0.721	0.845	0.335	0.692	0.743
AdvantageFlow(1.1)	0.987	0.957	0.778	0.861	0.290	0.685	0.749

Table 1: GenEval evaluation of AdvantageFlow, DiffusionNFT, and base model.

Trajectory-level RL. DDPO [Black et al., 2024] and DPOK [Fan et al., 2023] treat denoising as a finite-horizon Markov decision process and apply PPO-style updates to per-step Gaussian transitions. Flow-GRPO [Liu et al., 2025a] brings this idea to flow models by converting the sampling ODE into an SDE with tractable per-step likelihoods; later variants improve credit assignment and rollout efficiency [Xue et al., 2025b, He et al., 2025, Li et al., 2025a,b]. These methods optimize along the reverse trajectory, requiring credit assignment across many denoising steps. Forward-process RL avoids this by using the same prediction loss as pretraining.

Reward backpropagation. DRaFT [Clark et al., 2024], AlignProp [Prabhudesai et al., 2023], and Adjoint Matching [Domingo-Enrich et al., 2024] differentiate the reward through the sampler or an equivalent control objective. This is effective for differentiable rewards but does not directly apply to the black-box rule-based rewards, such as OCR, used in many text-to-image benchmarks.

Forward-process RL. The core idea - generate samples, score them, and retrain with the pretraining loss using reward-dependent weights - has appeared in several forms. Reward-weighted likelihood maximization [Lee et al., 2023, Peters and Schaal, 2007] and ORW-CFM-W2 [Fan et al., 2025b] weight the flow-matching loss by reward values. AWM [Xue et al., 2025a] uses advantage weighting. Centered Reward Distillation [Zhu et al., 2026] and AC-Flow [Fan et al., 2025a] also fit in this view. DiffusionNFT is the most closely related method [Zheng et al., 2026] as discussed in Sections D and 4.4.

7 Conclusions

We introduce AdvantageFlow, a forward-process RL algorithm for rectified flow models based on advantage-weighted least squares. The algorithm fits a local additive reward-improving distribution, where the rollout regularization reduces variance and keeps the per-sample quadratic loss strictly convex. We evaluate AdvantageFlow on image generation tasks, and show that it outperforms both Flow-GRPO and a state-of-the-art forward-process RL algorithm DiffusionNFT.

Limitations and future work. Our analysis is local and at a population level. We assume a centered population advantage and that the rollout predictor f_{old} is equal to the conditional mean under p_{old} . In practice, finite prompt groups, empirical reward normalization, clipped advantages, LoRA, and finite optimization are used. Therefore, our theory should be viewed as motivating and justifying our objective, rather than the exact description of the finite-sample training dynamics.

Our experiments are only with image generation in Stable Diffusion 3.5 Medium. The performance of AdvantageFlow depends on the quality of reward models, which we do not investigate. Learned reward models may be misspecified and rule-based reward models capture only a narrow aspect of image quality. Finally, the rollout and reference regularization strengths are hyper-parameters that need to be set, and a more complete theory for choosing them is needed.

References

- Michael S. Albergo, Nicholas M. Boffi, and Eric Vanden-Eijnden. Stochastic interpolants: A unifying framework for flows and diffusions. *arXiv preprint arXiv:2303.08797*, 2023.
- Shun-ichi Amari. Natural gradient works efficiently in learning. *Neural Computation*, 10(2):251–276, 1998.
- Jonathan Baxter and Peter Bartlett. Infinite-horizon policy-gradient estimation. *Journal of Artificial Intelligence Research*, 15:319–350, 2001.
- Kevin Black, Michael Janner, Yilun Du, Ilya Kostrikov, and Sergey Levine. Training diffusion models with reinforcement learning. In *ICLR*, 2024.
- George Casella and Christian Robert. Rao-Blackwellisation of sampling schemes. *Biometrika*, 83(1): 81–94, 1996.
- Kevin Clark, Paul Vicol, Kevin Swersky, and David J. Fleet. Directly fine-tuning diffusion models on differentiable rewards. In *ICLR*, 2024.
- Carles Domingo-Enrich, Michal Drozdal, Brian Karrer, and Ricky T. Q. Chen. Adjoint matching: Fine-tuning flow and diffusion generative models with memoryless stochastic optimal control. *arXiv preprint arXiv:2409.08861*, 2024.
- Patrick Esser, Sumith Kulal, Andreas Blattmann, Rahim Entezari, Jonas Muller, Harry Saini, Yam Levi, Dominik Lorenz, Axel Sauer, Frederic Boesel, Dustin Podell, Tim Dockhorn, Zion English, and Robin Rombach. Scaling rectified flow transformers for high-resolution image synthesis. In *Proceedings of the 41th International Conference on Machine Learning*, 2024.
- Jiajun Fan, Chaoran Cheng, Shuaike Shen, Xiangxin Zhou, and Ge Liu. Fine-tuning flow matching generative models with intermediate feedback. *arXiv preprint arXiv:2510.18072*, 2025a.
- Jiajun Fan, Shuaike Shen, Chaoran Cheng, Yuxin Chen, Chumeng Liang, and Ge Liu. Online reward-weighted fine-tuning of flow matching with Wasserstein regularization. In *ICLR*, 2025b.
- Ying Fan, Olivia Watkins, Yuqing Du, Hao Liu, Moonkyung Ryu, Craig Boutilier, Pieter Abbeel, Mohammad Ghavamzadeh, Kangwook Lee, and Kimin Lee. DPOK: Reinforcement learning for fine-tuning text-to-image diffusion models. In *NeurIPS*, 2023.
- Dhruba Ghosh, Hannaneh Hajishirzi, and Ludwig Schmidt. GenEval: An object-focused framework for evaluating text-to-image alignment. In *Advances in Neural Information Processing Systems 36*, 2023.
- Xiaoxuan He, Siming Fu, Yuke Zhao, Wanli Li, Jian Yang, Dacheng Yin, Fengyun Rao, and Bo Zhang. TempFlow-GRPO: When timing matters for GRPO in flow models. *arXiv preprint arXiv:2508.04324*, 2025.
- Jack Hessel, Ari Holtzman, Maxwell Forbes, Ronan Le Bras, and Yejin Choi. CLIPScore: A reference-free evaluation metric for image captioning. In *Proceedings of the 2021 Conference on Empirical Methods in Natural Language Processing*, 2021.
- Edward Hu, Yelong Shen, Phillip Wallis, Zeyuan Allen-Zhu, Yanzhi Li, Shean Wang, Lu Wang, and Weizhu Chen. LoRA: Low-rank adaptation of large language models. In *Proceedings of the 10th International Conference on Learning Representations*, 2022.
- Sham M. Kakade. A natural policy gradient. In *NeurIPS*, 2001.
- Yuval Kirstain, Adam Polyak, Uriel Singer, Shahbuland Matiana, Joe Penna, and Omer Levy. Pick-a-Pic: An open dataset of user preferences for text-to-image generation. In *Advances in Neural Information Processing Systems 36*, 2023.
- Kimin Lee, Hao Liu, Moonkyung Ryu, Olivia Watkins, Yuqing Du, Craig Boutilier, Pieter Abbeel, Mohammad Ghavamzadeh, and Shixiang Shane Gu. Aligning text-to-image models using human feedback. *arXiv preprint arXiv:2302.12192*, 2023.

- Junzhe Li, Yutao Cui, Tao Huang, Yinping Ma, Chun Fan, Yiming Cheng, Miles Yang, Zhao Zhong, and Liefeng Bo. MixGRPO: Unlocking flow-based GRPO efficiency with mixed ODE-SDE. *arXiv preprint arXiv:2507.21802*, 2025a.
- Yuming Li, Yikai Wang, Yuying Zhu, Zhongyu Zhao, Ming Lu, Qi She, and Shanghang Zhang. BranchGRPO: Stable and efficient GRPO with structured branching in diffusion models. *arXiv preprint arXiv:2509.06040*, 2025b.
- Yaron Lipman, Ricky T. Q. Chen, Heli Ben-Hamu, Maximilian Nickel, and Matt Le. Flow matching for generative modeling. In *ICLR*, 2023.
- Jie Liu, Gongye Liu, Jiajun Liang, Yangguang Li, Jiaheng Liu, Xintao Wang, Pengfei Wan, Di Zhang, and Wanli Ouyang. Flow-GRPO: Training flow matching models via online RL. *arXiv preprint arXiv:2505.05470*, 2025a.
- Xingchao Liu, Chengyue Gong, and Qiang Liu. Flow straight and fast: Learning to generate and transfer data with rectified flow. In *ICLR*, 2023.
- Zichen Liu, Changyu Chen, Wenjun Li, Penghui Qi, Tianyu Pang, Chao Du, Wee Sun Lee, and Min Lin. Understanding R1-Zero-like training: A critical perspective. In *Conference on Language Modeling*, 2025b.
- Remi Munos. Geometric variance reduction in Markov chains: Application to value function and gradient estimation. *Journal of Machine Learning Research*, 7:413–427, 2006.
- Jan Peters and Stefan Schaal. Reinforcement learning by reward-weighted regression for operational space control. In *ICML*, 2007.
- Mihir Prabhudesai, Anirudh Goyal, Deepak Pathak, and Katerina Fragkiadaki. Aligning text-to-image diffusion models with reward backpropagation. *arXiv preprint arXiv:2310.03739*, 2023.
- Yash Savani, Branislav Kveton, Yuchen Liu, Yilin Wang, Jing Shi, Subhojyoti Mukherjee, Nikos Vlassis, and Krishna Kumar Singh. Stepwise credit assignment for GRPO on flow-matching models. *arXiv preprint arXiv:2603.28718*, 2026.
- Zhihong Shao, Peiyi Wang, Qihao Zhu, Runxin Xu, Junxiao Song, Xiao Bi, Haowei Zhang, Mingchuan Zhang, Y. K. Li, Y. Wu, and Daya Guo. DeepSeekMath: Pushing the limits of mathematical reasoning in open language models. *arXiv preprint arXiv:2402.03300*, 2024.
- Richard Sutton, David McAllester, Satinder Singh, and Yishay Mansour. Policy gradient methods for reinforcement learning with function approximation. In *Advances in Neural Information Processing Systems 12*, pages 1057–1063, 2000.
- Masatoshi Uehara, Yulai Zhao, Tommaso Biancalani, and Sergey Levine. Understanding reinforcement learning-based fine-tuning of diffusion models: A tutorial and review. *arXiv preprint arXiv:2407.13734*, 2024.
- Ronald Williams. Simple statistical gradient-following algorithms for connectionist reinforcement learning. *Machine Learning*, 8(3-4):229–256, 1992.
- Xiaoshi Wu, Keqiang Sun, Feng Zhu, Rui Zhao, and Hongsheng Li. Human preference score: Better aligning text-to-image models with human preference. In *Proceedings of the IEEE/CVF International Conference on Computer Vision*, 2023.
- Shuchen Xue, Chongjian Ge, Shilong Zhang, Yichen Li, and Zhi-Ming Ma. Advantage weighted matching: Aligning RL with pretraining in diffusion models. *arXiv preprint arXiv:2509.25050*, 2025a.
- Zeyue Xue, Jie Wu, Yu Gao, Fangyuan Kong, Lingting Zhu, Mengzhao Chen, Zhiheng Liu, Wei Liu, Qiushan Guo, Weilin Huang, and Ping Luo. DanceGRPO: Unleashing GRPO on visual generation. *arXiv preprint arXiv:2505.07818*, 2025b.
- Kaiwen Zheng, Huayu Chen, Haotian Ye, Haoxiang Wang, Qinsheng Zhang, Kai Jiang, Hang Su, Stefano Ermon, Jun Zhu, and Ming-Yu Liu. DiffusionNFT: Online diffusion reinforcement with forward process. In *ICLR*, 2026. arXiv:2509.16117.

Yujie Zhou, Pengyang Ling, Jiazi Bu, Yibin Wang, Yuhang Zang, Jiaqi Wang, Li Niu, and Guangtao Zhai. Fine-grained GRPO for precise preference alignment in flow models. *arXiv preprint arXiv:2510.01982*, 2025.

Yuanzhi Zhu, Xi Wang, Stéphane Lathuilière, and Vicky Kalogeiton. Diffusion reinforcement learning via centered reward distillation. *arXiv preprint arXiv:2603.14128*, 2026.

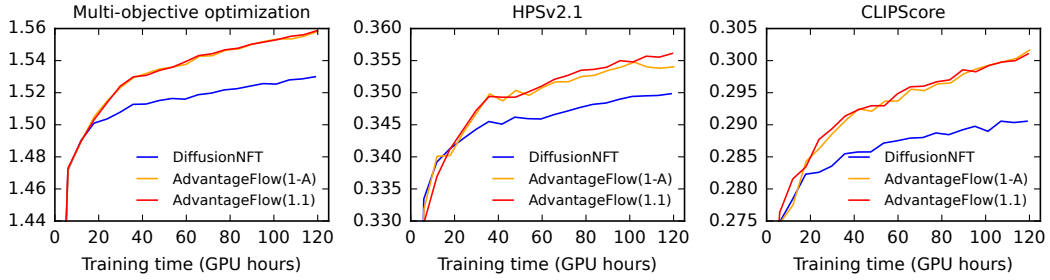


Figure 5: Evaluation of [AdvantageFlow](#) and [DiffusionNFT](#) on multi-objective optimization. We report the combined reward, as well as HPSv2.1 and CLIPScore. All rewards are measured on test sets and reported as a function of training time.



Figure 6: Images generated by [AdvantageFlow\(1.1\)](#) compared to [DiffusionNFT](#) and base model (Stable Diffusion 3.5 Medium) with cfg. We show improvements in object generation.

A Larger-Scale Experiment

Most results in Section 5 are computed in up to 35 H100 GPU hours. Now we report results up to 125 hours. To close the gap with the experiments in [Zheng et al. \[2026\]](#), we set the effective batch size to 512: 32 prompts with 16 samples per prompt. In this setting, both the number of prompts and samples are 1.5 times lower than in [Zheng et al. \[2026\]](#), and thus comparable.

All compared methods optimize the sum of PickScore, HPSv2.1, and CLIPScore, as in Figure 3a, and their rewards are shown in Figure 5. We observe more significant gains than before: both variants of [AdvantageFlow](#) attain the highest reward of [DiffusionNFT](#) in less than a third training time. This is likely caused by empirical loss functions being less noisy, since they are computed from 4 times more samples, and this pronounces differences between the different optimized objectives.

We show qualitative examples of generated images after training for 125 GPU hours next. Figure 6 shows improvements in object generation, Figure 7 shows improvements in counting and position understanding, and Figure 8 shows improvements in color understanding.

B Fisher–Rao Derivation

We prove Proposition 1, restated below for convenience.

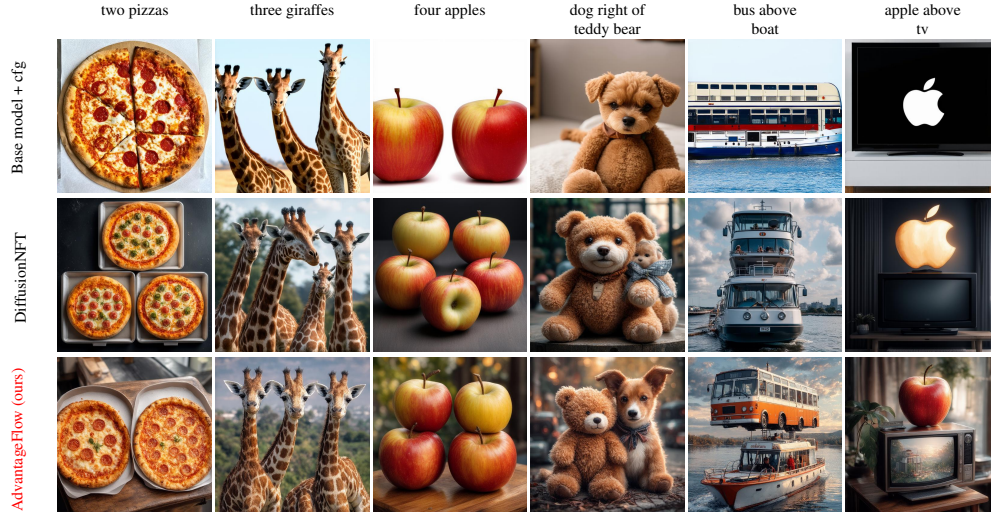


Figure 7: Images generated by [AdvantageFlow\(1.1\)](#) compared to [DiffusionNFT](#) and base model (Stable Diffusion 3.5 Medium) with cfg. We show improvements in counting and position understanding.



Figure 8: Images generated by [AdvantageFlow\(1.1\)](#) compared to [DiffusionNFT](#) and base model (Stable Diffusion 3.5 Medium) with cfg. We show improvements in color understanding.

Proposition 1 (restated). Fix a prompt c and let $F(p) = \mathbb{E}_p[r(\cdot, c)]$. Under the Fisher–Rao metric, the natural-gradient direction of F at $p = p_{\text{old}}(\cdot | c)$ is

$$\delta p(x_0) = A(x_0, c) p_{\text{old}}(x_0 | c), \quad A(x_0, c) = r(x_0, c) - \mathbb{E}_{p_{\text{old}}(\cdot | c)}[r(\cdot, c)].$$

A first-order step of size η yields the additive tilt $q_\eta(\cdot | c) = (1 + \eta A(\cdot, c)) p_{\text{old}}(\cdot | c)$ from Equation (9).

Proof. Let

$$F(p) = \mathbb{E}_p[r]. \tag{15}$$

For a perturbation δp of a density p , the probability constraint requires

$$\int \delta p(x) dx = 0. \tag{16}$$

The first variation of F is

$$\delta F = \int r(x) \delta p(x) dx. \quad (17)$$

Under the Fisher–Rao metric, tangent vectors are written as $\delta p(x) = u(x)p(x)$ with $\mathbb{E}_p[u] = 0$, and the inner product is

$$\langle u, v \rangle_p = \mathbb{E}_p[u(x)v(x)]. \quad (18)$$

The gradient direction u^* must satisfy

$$\mathbb{E}_p[u^*(x)u(x)] = \mathbb{E}_p[r(x)u(x)] \quad (19)$$

for every zero-mean tangent function u . Therefore

$$u^*(x) = r(x) - \mathbb{E}_p[r]. \quad (20)$$

At $p = p_{\text{old}}$, this gives the Fisher–Rao natural-gradient direction

$$\delta p(x) = A(x) p_{\text{old}}(x), \quad A(x) = r(x) - \mathbb{E}_{p_{\text{old}}}[r]. \quad (21)$$

A first-order step of size η gives

$$q_\eta(x) = p_{\text{old}}(x) + \eta A(x) p_{\text{old}}(x) = (1 + \eta A(x)) p_{\text{old}}(x). \quad (22)$$

□

C Two-Anchor Equivalence and Variance Reduction

We prove Proposition 2, restated below for convenience.

Proposition 2 (restated). Fix a prompt c and suppose $f_{\text{old}}(x_t, t, c) = \mathbb{E}_{x_0 \sim p_{\text{old}}(\cdot|c), \epsilon} [x_0 | x_t, t, c]$. Up to a θ -independent constant,

$$\mathbb{E}_{x_0 \sim p_{\text{old}}, \epsilon, t} [\|x_0 - f_\theta(x_t, t, c)\|_2^2] = \mathbb{E}_{x_0 \sim p_{\text{old}}, \epsilon, t} [\|f_{\text{old}}(x_t, t, c) - f_\theta(x_t, t, c)\|_2^2].$$

Moreover, the single-sample gradient of the right-hand side has no larger variance than that of the left-hand side.

Proof. Fix a prompt c and suppress it for brevity. Fitting the additive target gives

$$\mathcal{L}_{q_\eta}(\theta) = \mathbb{E}_{p_{\text{old}}, \epsilon, t} [(1 + \eta A(x_0)) \|x_0 - f_\theta(x_t, t)\|_2^2]. \quad (23)$$

Expanding,

$$\begin{aligned} \mathcal{L}_{q_\eta}(\theta) &= \mathbb{E}_{p_{\text{old}}, \epsilon, t} [\|x_0 - f_\theta(x_t, t)\|_2^2] \\ &\quad + \eta \mathbb{E}_{p_{\text{old}}, \epsilon, t} [A(x_0) \|x_0 - f_\theta(x_t, t)\|_2^2]. \end{aligned} \quad (24)$$

Assume

$$f_{\text{old}}(x_t, t) = \mathbb{E}_{p_{\text{old}}} [x_0 | x_t, t]. \quad (25)$$

Then

$$x_0 - f_\theta = (x_0 - f_{\text{old}}) + (f_{\text{old}} - f_\theta). \quad (26)$$

Taking squared norms and expectations,

$$\begin{aligned} \mathbb{E} \|x_0 - f_\theta\|_2^2 &= \mathbb{E} \|x_0 - f_{\text{old}}\|_2^2 + \mathbb{E} \|f_{\text{old}} - f_\theta\|_2^2 \\ &\quad + 2 \mathbb{E} \langle x_0 - f_{\text{old}}, f_{\text{old}} - f_\theta \rangle. \end{aligned} \quad (27)$$

The cross term vanishes because

$$\mathbb{E}[x_0 - f_{\text{old}} | x_t, t] = 0. \quad (28)$$

Therefore

$$\mathbb{E}_{p_{\text{old}}, \epsilon, t} [\|x_0 - f_\theta(x_t, t)\|_2^2] = \mathbb{E}_{p_{\text{old}}, \epsilon, t} [\|f_{\text{old}}(x_t, t) - f_\theta(x_t, t)\|_2^2] + C, \quad (29)$$

where C is independent of θ . Substituting and rescaling by $1/\eta$ gives

$$\mathcal{L}_{\text{AFM}}(\theta) = \mathbb{E}_{p_{\text{old}}, \epsilon, t} \left[A(x_0) \|x_0 - f_\theta(x_t, t)\|_2^2 + \frac{1}{\eta} \|f_\theta(x_t, t) - f_{\text{old}}(x_t, t)\|_2^2 \right], \quad (30)$$

up to a θ -independent constant.

Variance reduction. Let

$$g_{\text{sample}} = \nabla_{\theta} \|x_0 - f_{\theta}(x_t, t)\|_2^2, \quad g_{\text{rollout}} = \nabla_{\theta} \|f_{\text{old}}(x_t, t) - f_{\theta}(x_t, t)\|_2^2$$

be the single-sample gradients of the two terms. Since $f_{\text{old}}(x_t, t) = \mathbb{E}[x_0 | x_t, t]$,

$$g_{\text{rollout}} = \mathbb{E}[g_{\text{sample}} | x_t, t]. \quad (31)$$

The Rao–Blackwell inequality gives

$$\text{Var}(g_{\text{rollout}}) \leq \text{Var}(g_{\text{sample}}). \quad (32)$$

□

D DiffusionNFT Algebra

We prove the **DiffusionNFT** connection stated in Section 4.4.

Proposition 3 (**DiffusionNFT** as a special case of **AdvantageFlow**). *Let $r(x_0, c) \in [0, 1]$ be a normalized optimality score and $A(x_0, c) = 2r(x_0, c) - 1$. The **DiffusionNFT** branch loss, after replacing velocity losses with prediction losses and dropping θ -independent constants, equals*

$$\beta A(x_0, c) \|x_0 - f_{\theta}(x_t, t, c)\|_2^2 + \beta(\beta - A(x_0, c)) \|f_{\theta}(x_t, t, c) - f_{\text{old}}(x_t, t, c)\|_2^2,$$

corresponding to the **AdvantageFlow** objective (5) with $\lambda = 0$ and rollout regularization schedule $\gamma_{\text{NFT}}(A) = \beta(\beta - A(x_0, c))$.

Proof. We work in velocity space, since that is how **DiffusionNFT** states its objective.

Let v be the forward-process velocity target, let v_{old} be the rollout model, and let v_{θ} be the trainable model. **DiffusionNFT** defines positive and negative branches

$$v_{\theta}^+ = (1 - \beta)v_{\text{old}} + \beta v_{\theta}, \quad v_{\theta}^- = (1 + \beta)v_{\text{old}} - \beta v_{\theta}. \quad (33)$$

Let $r \in [0, 1]$ be the normalized optimality score and define $A(x_0, c) = 2r(x_0, c) - 1$. The branch loss is

$$\ell_{\text{NFT}} = r \|v_{\theta}^+ - v\|_2^2 + (1 - r) \|v_{\theta}^- - v\|_2^2. \quad (34)$$

Set $d = v_{\theta} - v_{\text{old}}$ and $e = v_{\text{old}} - v$. Then

$$v_{\theta}^+ - v = e + \beta d, \quad v_{\theta}^- - v = e - \beta d. \quad (35)$$

Expanding,

$$\ell_{\text{NFT}} = \|e\|_2^2 + \beta^2 \|d\|_2^2 + 2\beta A(x_0, c) \langle e, d \rangle. \quad (36)$$

Now consider the two-anchor expression

$$A(x_0, c) \|v_{\theta} - v\|_2^2 + (\beta - A(x_0, c)) \|v_{\theta} - v_{\text{old}}\|_2^2. \quad (37)$$

Since $v_{\theta} - v = e + d$, this equals

$$A(x_0, c) \|e\|_2^2 + \beta \|d\|_2^2 + 2A(x_0, c) \langle e, d \rangle. \quad (38)$$

Multiplying by β gives

$$\beta A(x_0, c) \|e\|_2^2 + \beta^2 \|d\|_2^2 + 2\beta A(x_0, c) \langle e, d \rangle. \quad (39)$$

This differs from Equation (36) only by $(1 - \beta A(x_0, c)) \|e\|_2^2$, which is independent of v_{θ} . Therefore, after dropping constants,

$$\ell_{\text{NFT}} \equiv \beta A(x_0, c) \|v_{\theta} - v\|_2^2 + \beta(\beta - A(x_0, c)) \|v_{\theta} - v_{\text{old}}\|_2^2. \quad (40)$$

To pass from velocity space to prediction space, use

$$f_{\theta}(x_t, t, c) = x_t - tv_{\theta}(x_t, t, c), \quad f_{\text{old}}(x_t, t, c) = x_t - tv_{\text{old}}(x_t, t, c),$$

and let $v = \epsilon - x_0$ be the forward-process velocity target. Then

$$x_0 - f_{\theta}(x_t, t, c) = t(v_{\theta} - v), \quad f_{\theta}(x_t, t, c) - f_{\text{old}}(x_t, t, c) = -t(v_{\theta} - v_{\text{old}}).$$

Thus, after moving to the prediction-loss by multiplying the velocity-space objective by t^2 , we have

$$t^2 \|v_{\theta} - v\|_2^2 = \|x_0 - f_{\theta}(x_t, t, c)\|_2^2, \quad t^2 \|v_{\theta} - v_{\text{old}}\|_2^2 = \|f_{\theta}(x_t, t, c) - f_{\text{old}}(x_t, t, c)\|_2^2.$$

Substituting these identities into the velocity-space expression gives Equation (14). Thus **DiffusionNFT** corresponds to the advantage-dependent schedule

$$\gamma_{\text{NFT}}(A) = \beta(\beta - A(x_0, c)). \quad (41)$$

For $\beta = 1$, this becomes $\gamma_{\text{NFT}}(A) = 1 - A(x_0, c)$. □